Validation and sensitivity tests on improved parametrizations of a land surface process model (LSPM) in the Po Valley (*)

C. CASSARDO ([1]), E. CARENA ([2]) and A. LONGHETTO ([2])

([1]) *Dipartimento di Scienze e Tecnologie Avanzate, Università di Torino Sede di Alessandria, Italy*
([2]) *Dipartimento di Fisica Generale "Amedeo Avogadro", Universià di Torino - Torino, Italy*

(ricevuto il 18 Agosto 1997; approvato il 16 Settembre 1997)

Summary. — The Land Surface Process Model (LSPM) has been improved with respect to the 1st version of 1994. The modifications have involved the parametrizations of the radiation terms and of turbulent heat fluxes. A parametrization of runoff has also been developed, in order to close the hydrologic balance. This 2nd version of LSPM has been validated against experimental data gathered at Mottarone (Verbania, Northern Italy) during a field experiment. The results of this validation show that this new version is able to apportionate the energy into sensible and latent heat fluxes. LSPM has also been submitted to a series of sensitivity tests in order to investigate the hydrological part of the model. The physical quantities selected in these sensitivity experiments have been the initial soil moisture content and the rainfall intensity. In each experiment, the model has been forced by using the observations carried out at the synoptic stations of San Pietro Capofiume (Po Valley, Italy). The observed characteristics of soil and vegetation (not involved in the sensitivity tests) have been used as initial and boundary conditions. The results of the simulation show that LSPM can reproduce well the energy, heat and water budgets and their behaviours with varying the selected parameters. A careful analysis of the LSPM output shows also the importance to identify the effective soil type.

PACS 92.60.Fm – Boundary layer structure and processes.
PACS 92.60.Jq – Water in the atomosphere (humidity, clouds, evaporation, precipitation).

1. – Introduction

Most of the work carried out in the recent years on the numerical models of atmospheric circulation has been addressed to the improvement of soil-vegetation-atmosphere parametrizations. In fact, numerical simulations performed with limited

(*) The authors of this paper have agreed to not receive the proofs for correction.

area models (LAM) and general circulation models (GCM) have demonstrated that predicted climates are sensitive to surface parameters, and that representation of land surface processes is one of the most challenging aspects of the present climate change simulations (Sellers *et al.*, 1989; Henderson-Sellers and Pitman, 1992).

It is well known that, basically, the atmosphere interacts with the terrestrial surface in three ways: with the exchange of radiation between the two systems, with the drag force exerted by the roughness elements (mainly vegetation) and, finally, through the availability of moisture for evapotranspiration and through the control exerted by the vegetation on its release.

To properly describe the interactions between the land surface and the atmospheric boundary layer, one must adequately describe heat and moisture transport at the surface and sub-surface (Ek and Cuenca, 1994). In fact, the soil-vegetation system behaves as a water reservoir whose content varies in response to fluctuating supplies and demands, and a critical parameter that affects evaporation is the effective water-holding capacity of the soil (Milly and Dunne, 1994).

Moreover, the determination of the partition between sensible and latent heat flux is crucial to good prediction of precipitation; unrealistically strong inversions, due to an incorrect representation of the soil moisture field, can cap the boundary layer humidity and produce excessive heating (as in the case described by Beljaars *et al.*, 1994). It must in fact be remembered that, with the correct radiative forcing at the surface, the land surface schemes are also largely responsible for the quality of the model-produced near-surface weather quantities, such as screen level temperature and dew point, and low-level cloudiness (Viterbo and Beljaars, 1995). Furthermore, as Milly and Dunne (1994) pointed out, the soil moisture reservoir is a crucial factor in climate and numerical weather prediction models.

From all of the above considerations it is clear that a numerical model of atmospheric circulation requires an adequate group of physical parametrizations regarding the interactions between soil, vegetation and atmosphere, in which each process must be modelled on the basis of the underlying physical principles (Abramopoulos *et al.*, 1988, and Verstraete and Dickinson, 1986). Obviously, the detail in these calculations should be restricted to an appropriate level for use in GCM or LAM, to avoid the common problem of model computer time. In addition, if we wish to perform realistic climatic predictions, it may be necessary to include an interactive biosphere, as discussed by Henderson-Sellers and Pitman (1992) and by Zhang (1994).

On the mesoscale, and on the scale of plant-atmosphere interactions, the lack of experimental data for testing model calculations makes the validation of the above parametrizations a difficult task (Tjernstrom, 1989). Within the Project for Intercomparison of Land Surface Parametrization Schemes (PILPS, Henderson-Sellers *et al.*, 1993), it has been suggested that model tests should proceed in two stages: on the one hand, the model validation, on the other hand, the sensitivity analysis.

A biospheric scheme can be tested separately from the GCM or LAM, in order to verify its absolute skill (Bosilovich and Sun, 1995); this kind of model checking is called the “stand-alone” (or “off-line”) procedure: its experimental framework is extremely simple, and permits checking of a land surface scheme in isolation from other deficiencies in the GCM or LAM and complex feedback with atmospheric forcing. Furthermore, this procedure can be justified by noting that all surface layer parametrizations are based on concepts that have local meaning, *i.e.* relationships between local fluxes and gradients within the surface layer (Jacquemin and Nohilan, 1990).

In this paper, we will describe the improvements carried out on the first version of LSPM (sect. **2**). We have applied the above-mentioned model checking strategy by performing validation and sensitivity test on LSPM. Section **3** describes the validation experiment. In sect. **4** the experimental setup for sensitivity tests is described. In sect. **5** the boundary and initial conditions used in the sensitivity experiments are presented. Finally, sect. **6** illustrates the results of the sensitivity experiments.

2. – The LSPM

The model used in this work is an improved version of the Land Surface Process Model (LSPM) of Cassardo *et al.* (1995a, hereafter C95). The schematic structure of LSPM includes an atmospheric layer above the vegetation (up to a reference height z_a), the canopy (considered as a uniform layer characterised by the following parameters: vegetation cover *veg*, height h, leaf area index LAI, albedo a_c, minimum stomatal resistance r_{min}, leaf dimension d_0, emissivity ε_c and root depth d_r), and the soil (described by a multilayer scheme and characterised by the parameters: thermal conductivity λ, hydraulic conductivity $K_{\eta j}$, with $j = 1, 5$ number of soil layers, soil surface albedo α_g, porosity η_s, permanent wilting point W_{wilt}, dry volumetric heat capacity ϱc_s and emissivity ε_g). A list of all the parameters and variables used by the LSPM, together with their symbol and units, is given in table I.

The initial conditions assumed in the experiments carried out in this work for temperature and moisture in the five soil layers are shown in table II. The boundary conditions are the atmospheric data measured at reference height z_a, *i.e.*: air temperature T_a, air specific humidity q_a, wind velocity u_a, incoming short-wave and long-wave radiation $R^{\downarrow}_{SW}$ and $R^{\downarrow}_{LW}$ (the former, if unavailable, can be parametrized as a function of the cloud cover by a specific subroutine of the LSPM code), air pressure p_a and precipitation rate P_0.

LSPM calculates the thermal, energetic and hydrologic exchanges among the components of the atmosphere-vegetation-soil system; the fluxes are evaluated with an electric analogue scheme using five resistances: two aerodynamic (r_a above the vegetation, and r_d above the bare soil), one laminar (r_b over the leaves), and two related to the water vapour transfer (r_c for the canopy and r_{soil} for the soil). Finally, all global variables are expressed as weighted averages between bare soil and canopy components by using *"veg"* as the weighting function.

The improvements carried out on LSPM involved the evaluation of the radiation flux, the sensible and latent heat fluxes and the parametrization of surface runoff and underground drainage, and were carried out on the LSPM C95 version, in order to improve and extend the consistency of its parametrizations to some asymptotic conditions of land surface. All modifications are described in the following subsections. This new version of LSPM has already be used in Ruti *et al.* (1997) in a validation and model intercomparison experiment.

2˙1. *Radiation flux formulation.* – The net radiation flux within the canopy has been evaluated as the balance between the short-wave (R_{swc}) and long-wave (T_{lwc}) radiation fluxes above the canopy (Deardorff, 1978; McCumber and Pielke, 1981):

$$R_{nc} = R^{\downarrow}_{swc} - R^{\uparrow}_{swc} + R^{\downarrow}_{lwc} - R^{\uparrow}_{lwc}\,, \tag{1}$$

TABLE I. – *List of symbols quoted in the paper.*

C_c'	dimensional coefficient in the parametrization for r_b	$s^{0.5}\,m^{-1}$
C_{DC}	drag coefficient for canopy	—
C_{DS}	drag coefficient in canopy air-space	—
d_0	leaf dimension	m
d_j, $j = 1, 5$	soil layer depths	m
d_r	root depth	m
E_a	evaporation flux at reference height z_a	Wm^{-2}
E_c	evaporation flux from canopy surface	Wm^{-2}
EG	evaporation rate from bare soil	Wm^{-2}
EFW	evaporation flux from wet canopy	Wm^{-2}
f_h	relative humidity of air over soil surface	—
h	vegetation height	m
H	sensible heat flux	Wm^{-2}
H_a	sensible heat flux at reference height z_a	Wm^{-2}
H_c	sensible heat flux at canopy surface	Wm^{-2}
H_g	sensible heat flux at bare soil surface	Wm^{-2}
$K_{\eta sj}$, $j = 1, 5$	saturated hydraulic conductivity of soil in the j-th layer	ms^{-1}
LAI	leaf area index	$m^2\,m^{-2}$
LE	latent heat flux	Wm^{-2}, mm
m_j, $j = 1, 2$	coefficients in the parametrization for r_{soil}	—
p_a	air pressure at reference hight z_a	Pa
P_g	precipitation rate at soil surface	ms^{-1}
P_0	observed precipitation rate at reference height z_a	ms^{-1}
PC	precipitation code (see sect. **3**)	—
q_a	specific humidity of air reference height z_a	$kgkg^{-1}$
q_{ac}	specific humidity in canopy air-space	$kgkg^{-1}$
QG	conductive flux at soil-atmosphere interface	Wm^{-2}
R	turbidity factor (Page, 1986)	—
r_a	aerodynamic resistance above vegetation	sm^{-1}
r_b	laminar resistance over leaves	sm^{-1}
r_c	canopy stomatal resistance	sm^{-1}
r_d	aerodynamic resistance above bare soil	sm^{-1}
r_{soil}	bare soil resistance to evaporation	sm^{-1}
r_{min}	minimum stomatal resistance	sm^{-1}
r_s	surface runoff	ms^{-1}
r_u	drainage or underground runoff	ms^{-1}
r_u^*	threshold value of drainage (appendix A)	ms^{-1}
RN	net radiation at reference height z_a	Wm^{-2}
$R_{lw}^{\downarrow}$	downward incoming long-wave radiation	Wm^{-2}
$R_{lwc}^{\downarrow}$	downward long-wave radiation within canopy layer	Wm^{-2}
$R_{lwc}^{\uparrow}$	upward long-wave radiation within canopy layer	Wm^{-2}
$R_{lwv}^{\downarrow}$	downward long-wave radiation below canopy layer	Wm^{-2}
$R_{lwv}^{\uparrow}$	upward long-wave radiation below canopy layer	Wm^{-2}
$R_{lwu}^{\downarrow}$	downward long-wave radiation above canopy layer	Wm^{-2}
$R_{lwu}^{\uparrow}$	upward long-wave radiation above canopy layer	Wm^{-2}
$R_{sw}^{\downarrow}$	downward incoming solar radiation	Wm^{-2}
$R_{swc}^{\downarrow}$	downward short-wave radiation within canopy layer	Wm^{-2}
$R_{swc}^{\uparrow}$	upward short-wave radiation within canopy layer	Wm^{-2}
$R_{sw}^{\downarrow\,max}$	maximum value of $R_{SW}^{\downarrow}$	Wm^{-2}
s_a, s_b, s_c, s_d, s_s	conductances (defined in subsect. **2**·2)	ms^{-1}

TABLE I. (*Continued*)

ST	soil type (according to Clapp and Hornberger, 1978)	—
T_a	air temperature at reference heigt z_a	°C
T_{ac}	temperature in canopy air-space	°C
T_c	canopy temperature	°C
T_j, $j = 1, 5$	soil temperature in the j-th layer	°C
T_j^i, $j = 1, 5$	initial value of soil temperature in the j-th layer	°C
TR	transpiration heat flux	Wm^{-2}
u_{ac}	wind velocity in canopy air-space	ms^{-1}
veg	vegetation fractional cover	—
v_a	wind velocity at reference height z_a	ms^{-1}
v_{min}, v_{max}	threshold wind velocity for haze formation (Cassardo *et al.*, 1995a)	ms^{-1}
W_c	wet fraction of canopy	—
W_j, $j = 1, 5$	relative soil moisture in the j-th layer	—
W_j^i, $j = 1, 5$	initial value of the relative soil moisture in the j-th layer	—
W_s	average relative soil moisture in root layer	—
W_{wilt}	relative wilting point	—
W_*	initial value of the relative soil moisture for "loam" soil	—
$water$	total soil water content	cm
z_a	reference height (screen level)	m
z_{ac}	canopy-air-space height	m
a_c	canopy albedo	—
a_g	soil albedo	—
ε_a	atmospheric emissivity	—
ε_c	canopy emissivity	—
ε_g	bare soil emissivity	—
η_{sj}	saturated volumetric water content or porosity of the j-th soil layer	—
η_j	volumetric water content of the soil in the j-th soil layer	—
λ	thermal conductivity of soil	$Wm^{-1}K^{-1}$
ϱc_s	thermal capacity of soil	$Jkg^{-1}K^{-1}$
σ	Boltzmann constant	$Wm^{-2}K^{-1}$
ψ_{sj}	saturated moisture potential of the j-th soil layer	m

TABLE II. – *Reference initial and boundary conditions assumed for* LSPM *in the sensitivity experiments carried out on* LSPM.

Initial condition	Sens-itivity	Mot-tarone	Boundary conditions	Sens-itivity	Mot-tarone	Boundary conditions	Sens-itivity	Mot-tarone
T_1 (°C)	2.0	13.2	veg	0.90	0.90	ε_g	0.96	0.96
T_2 (°C)	3.0	13.2	d_0 (m)	0.02	0.02	z_a (m)	2.0	2.0
T_3 (°C)	5.0	13.2	α_c	0.28	0.28	v_{min} (ms^{-1})	2.0	2.0
T_4 (°C)	7.0	13.2	r_{min} (sm^{-1})	200	200	v_{max} (ms^{-1})	5.0	5.0
T_5 (°C)	10.0	13.2	LAI ($m^2\ m^{-2}$)	2	2	d_1 (m)	0.04	0.04
W_1	0.58	0.58	h (m)	0.10	0.10	d_2 (m)	0.12	0.12
W_2	0.58	0.58	ε_c	0.96	0.96	d_3 (m)	0.44	0.44
W_3	0.58	0.58	R_{SW}^{max} (Wm^{-2})	1000	1000	d_4 (m)	1.72	1.72
W_4	0.58	0.58	d_r (m)	0.10	0.10	d_5 (m)	6.84	6.84
W_5	0.58	0.58	R	−0.02	−0.02	ST	5 (loam)	5 (loam)

where the four terms have been recalculated (with respect to the C95 expression) as

$$R^{\downarrow}_{\mathrm{swc}} = veg R^{\downarrow}_{\mathrm{sw}} \,, \tag{2a}$$

$$R^{\uparrow}_{\mathrm{swc}} = veg \alpha_{\mathrm{c}} R^{\downarrow}_{\mathrm{sw}} \,, \tag{2b}$$

$$R^{\downarrow}_{\mathrm{lwc}} = veg (R^{\downarrow}_{\mathrm{lwu}} - R^{\downarrow}_{\mathrm{lwv}}) \,, \tag{2c}$$

$$R^{\uparrow}_{\mathrm{lwc}} = veg (R^{\uparrow}_{\mathrm{lwu}} - R^{\uparrow}_{\mathrm{lwv}}) \,, \tag{2d}$$

with

$$R^{\downarrow}_{\mathrm{lwu}} = \varepsilon_{\mathrm{a}} \sigma T_{\mathrm{a}}^4 \,, \tag{3a}$$

$$R^{\uparrow}_{\mathrm{lwu}} = \varepsilon_{\mathrm{c}} \sigma T_{\mathrm{c}}^4 + (1 - \varepsilon_{\mathrm{c}}) R^{\downarrow}_{\mathrm{lw}} \,, \tag{3b}$$

$$R^{\downarrow}_{\mathrm{lwv}} = \frac{\varepsilon_{\mathrm{c}} \sigma T_{\mathrm{c}}^4 + (1 - \varepsilon_{c}) \sigma T_1^4}{\varepsilon_{\mathrm{c}} + \varepsilon_{\mathrm{g}} - \varepsilon_{\mathrm{c}} \varepsilon_{\mathrm{g}}} \,, \tag{3c}$$

$$R^{\uparrow}_{\mathrm{lwv}} = \frac{\varepsilon_{\mathrm{g}} \sigma T_1^4 + (1 - \varepsilon_{\mathrm{g}}) \sigma T_{\mathrm{c}}^4}{\varepsilon_{\mathrm{c}} + \varepsilon_{\mathrm{g}} - \varepsilon_{\mathrm{c}} \varepsilon_{\mathrm{g}}} \,. \tag{3d}$$

2˙2. *Turbulent heat flux formulations.* – In order to carry out the sensitivity experiments on vegetation cover, we have modified the turbulent flux formulations used in the C95 version of LSPM. The new formulations are more consistent in the extreme limit $veg \to 0$ and $veg \to 1$. We overlooked these corrections in C95 because they produced negligible effects on the validation, the vegetation cover being fixed and close to 1. In the sensitivity experiments, on the contrary, the effects produced in the output data cannot be considered negligible, because vegetation cover can assume the extremal values of 0 or 1.

The formulations of the five resistances involved in the expressions for the sensible and latent heat fluxes (eqs. 31 to 33, 35 through 39 in C95) are now given by

$$r_a = \frac{veg}{C_{D\mathrm{c}} y_{\mathrm{ac}}} \,, \tag{4a}$$

$$r_b = \frac{C_{\mathrm{c}}}{LAI} \left(\frac{d_0}{u_{\mathrm{ac}}} \right)^{0.5} , \tag{4b}$$

$$r_c = \frac{r_{\min}}{LAI} \left[\frac{R^{\downarrow}_{\mathrm{sw\,max}}}{R^{\downarrow}_{\mathrm{sw}} + R^{\downarrow}_{\mathrm{sw\,max}}} + \left(\frac{W_{\mathrm{wilt}}}{W_{\mathrm{s}}} \right)^2 \right], \tag{4c}$$

$$r_d = \frac{1}{D_{D\mathrm{s}} u_{\mathrm{ac}}} \,, \tag{4d}$$

$$r_{\mathrm{soil}} = m_1 + m_2 W_1^{-2} \,, \tag{4e}$$

where all W quantities are relative humidities, *i.e.* ratios between volumetric water soil content η and soil porosity η_{s}.

The equations expressing the principle of "energy conservation" in the "electric node analogy" relative to the canopy air space z_{ac} level (eqs. 34 and 40 in C95) change, respectively, to

(5*a*) $$H_a = veg\, H_c + (1 - veg)\, H_g ,$$

(5*b*) $$E_a = veg\, E_c + (1 - veg)\, EG .$$

The values of temperature T_{ac} and specific humidity q_{ac} in the canopy air space level can then be computed from eqs. (5*a*), (5*b*), and eqs. 31-33 and 35-39 of C95, giving

(6*a*) $$T_{ac} = \frac{veg\, s_b\, T_c + (1 - veg)\, s_d\, T_g + s_a\, T_a}{veg\, s_s + (1 - veg)\, s_d + s_a} ,$$

(6*b*) $$q_{ac} = \frac{veg\, s_c\, q_s(T_c) + (1 - veg)\, s_s\, f_h\, q_s(T_g) + s_a\, q_a}{veg\, s_c + (1 - veg)\, s_s + s_a} ,$$

where we have used the conductances

$$s_a = r_a^{-1}, \quad s_b = 2\, r_b^{-1}, \quad s_c = \left(\frac{W_c}{r_b} + \frac{1 - W_c}{r_b + r_c} \right) \quad s_d = r_d^{-1} \text{ and } s_s = (r_d + r_{soil})^{-1}.$$

2·3. *Calculations of surface runoff and underground drainage.* – In order to test the ability of the model to simulate all the hydrological budget components, information regarding the runoff and drainage is needed. Runoff processes are extremely complex, depending on the soil profile, soil type, vegetation cover and type, land morphology, underlying geology and hydrological history of the soil. The runoff-generating mechanisms can be summarised as: "Hortonian runoff" (when local rainfall intensity exceeds surface infiltration rate), "saturation excess" (when soil is saturated and cannot accept anymore water), "saturation-through-flow" (caused by a horizontal irregular distribution of orography or water table into the soil). The commonly used parametrizations assume a non-zero instantaneous runoff only during rainfall or snowmelt, under conditions of high soil moisture concentrations. Such an approach is realistic, but empirical, because it is not directly related to any physical processes (Warrilow *et al.*, 1986), although both Hortonian and saturation excess could be considered to be relevant mechanisms.

According to these considerations, we have evaluated as surface runoff the amount of water that, during a precipitation event (or drainage from foliage), is not stored into the soil because it is larger than the soil infiltration capacity.

To take into account subgrid space variability of rainfall intensity and runoff in the parametrization of runoff itself, the infiltration capacity of soil has been assumed to depend on precipitation rate at the soil surface (P_g) and on the soil saturated hydraulic conductivity ($K_{\eta s1}$); this dependence has been obtained by modifying the empirical relation of Manley (1977), valid only when precipitation rates are lower than $K_{\eta s1}$, using a suggestion from Dingman (1994, chapt. 6). In conclusion, we used the following

parametrization for surface runoff r_s,

$$(7a)\qquad \begin{cases} r_s = \dfrac{P_g^2}{2K_{\eta s1}} & \text{if } P_g < K_{\eta s1}, \\ r_s = 0.5K_{\eta s1} & \text{if } K_{\eta s1} \leqslant P_g \leqslant 1.5K_{\eta s1}, \\ r_s = P_g - K_{\eta s1} & \text{if } P_g > 1.5K_{\eta s1}. \end{cases}$$

Furthermore, because in the case of high rainfall the water accumulated in a time step should be larger than the soil availability (due to the finite integration time), we assumed that the relative soil moisture remains lower than or equal to 1, and we took as surface runoff the value

$$(7b)\qquad r_s = \eta_{s1} d_1 (W_1 - 1) \qquad \text{if } W_1 > 1 .$$

The surface runoff has then been calculated as the sum of the values derived from eqs. (7*a*) and (7*b*).

The drainage of water (due to gravity) in the lowest soil layer, or underground runoff, r_u, has been simply evaluated by taking into account the soil hydraulic conductivity of this layer, *i.e.*

$$(8)\qquad r_u = K_{\eta 5}$$

as is commonly done (Sellers *et al.*, 1986; Dickinson *et al.*, 1986).

3. – Validation of LSPM on Mottarone data

The validation of the LSPM version presented in this paper has been performed using the data coming from the field experiment carried out in Mottarone station. This station is located near the top of the Mottarone mountain, located between the Orta and Maggiore lakes in the province of Verbania, in Piedmont (Northern Italy), at an approximative heigth of 1400 m a.s.l. In the period from 15th to 27th September, 1994, a field experiment has been performed, with the aim to collect turbulent fluxes data in a orographically complex environment. Some traditional sensors (for the measurements of air temperature and humidity, pressure, net and global radiation, precipitation) and fast-response sensors (sonic anemometers and fluxmeters) were installed on a grass field (with a vegetation cover of about 90%), located near the forests, at the base of the mountain top. The turbulent heat fluxes have been evaluated from the sonic anemometer output by using the method described in Cassardo *et al.* (1995b). The soil type near the station has been assumed to belong to the class of loam. The values of the initial conditions assumed for the simulation have been reported in table II. Regarding the soil moisture initial profile, the costant value of 0.58 (expressed in units of porosity) has been used. The “model spinup problems” have not been taken into consideration during this simulation, because in the field experiment period the precipitation was much intense. Then, as will be stressed in subsect. **6**·3, the upper soil layers were almost wet in all period, while the wetness of the lowest soil layers was not important as regards to this short-time simulation.

In figs. 1-4 the results of this validation are shown. The net radiation (*RN*, fig. 1) is well represented by LSPM both in sunny and in cloudy conditions. The predictions are close to the observations during day- and night-time, and only some maxima are

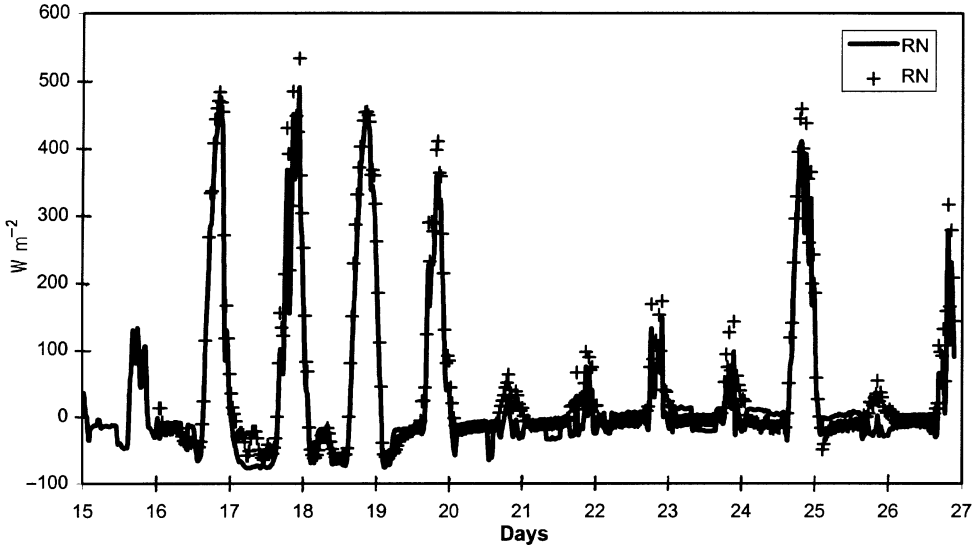

Fig. 1. – Validation experiment on Mottarone: net radiation (*RN*) predicted by LSPM (solid line) and observed (crosses), in Wm^{-2}. Units on abscissae are the days of the field experiment, starting from 15th September 1994.

underestimated. In spite of the fact that global (solar) radiation is used to force the model, the empirical radiative package used by LSPM (and mainly based on Page, 1986) allow a quite good representation of the effective radiation.

Sensible heat flux (*H*, fig. 2) is also well represented (except during day 25th, in which LSPM underestimates the observation). The diurnal range of variation during

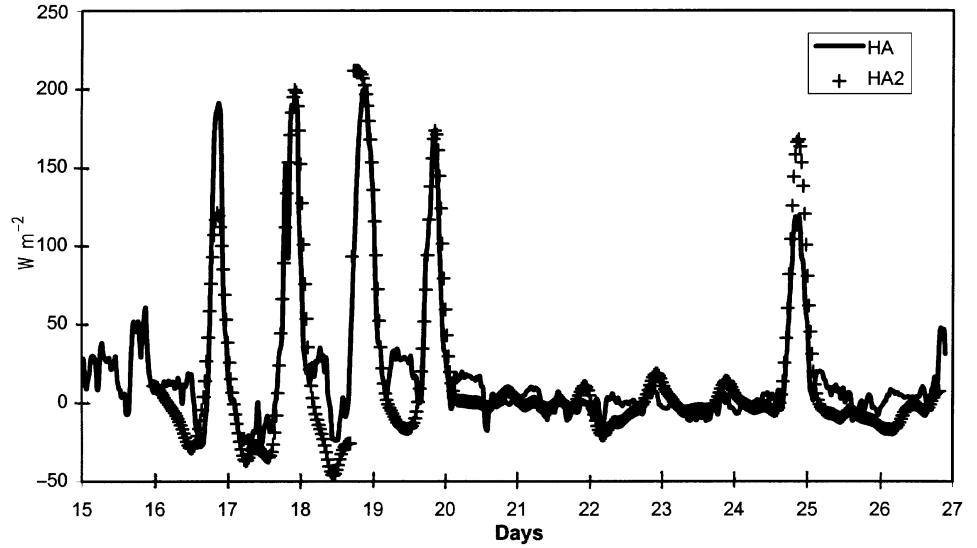

Fig. 2. – As in fig. 1 but for sensible heat flux (*H*), in Wm^{-2}.

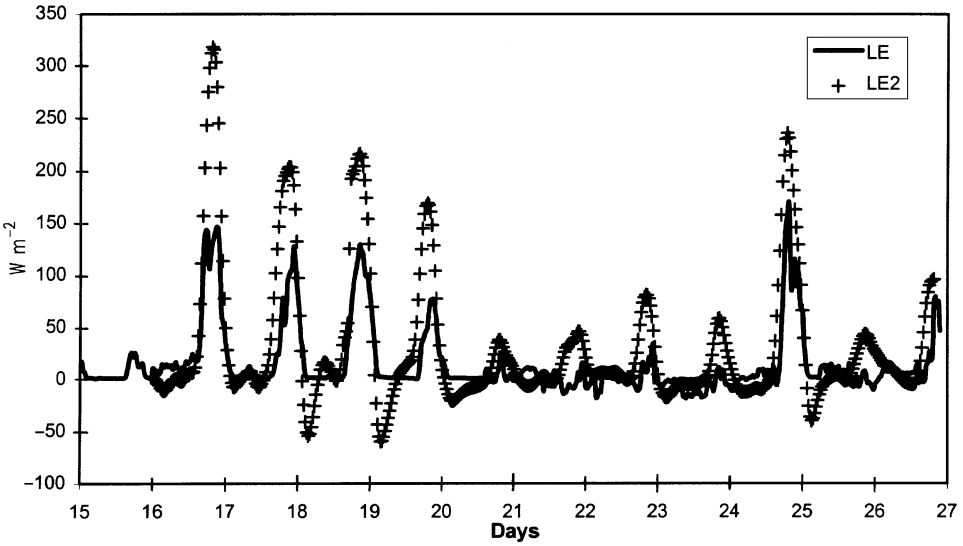

Fig. 3. – As in fig. 1 but for latent heat flux (*LE*), in Wm^{-2}.

sunny and rainy days is captured with high accuracy. Also the variations of latent heat fluxes (*LE*, fig. 3) are well represented in phase, but in this case LSPM tends to underestimate the positive (diurnal) and negative (nocturnal) peaks in all the days of the simulation. The reason for this underestimation could be searched, perhaps, in the parametrization of the canopy resistance in these extremal conditions (due to the orographically complex environment). These underestimations of evapotranspiration are obviously reflected on the values of conductive heat flux (that is evaluated by LSPM

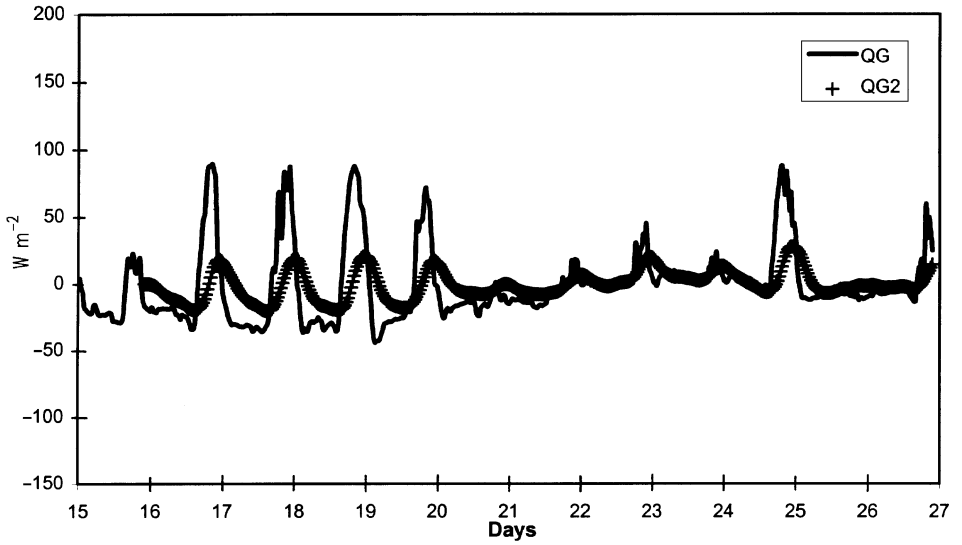

Fig. 4. – As in fig. 1 but for ground-atmosphere heat flux (*QG*), in Wm^{-2}.

through the balance equation) and then on those of soil temperature (not shown). Figure 4 reports the ground-atmosphere heat flux (*QG*) predicted by LSPM, compared with the one "measured ([1])" at Mottarone. As is evident, the same underestimations present in the evapotranspiration can be found (with opposite sign) in *QG* values. These values cause an exhaggeration of the soil temperature daily cycle that propagates into the soil. Even if they seem not to cause a systematic error (because their mean values are about zero), it is clear that in the further works these problems must be taken into consideration.

4. – Setup and results of the sensitivity experiments

The parameters used in the sensitivity experiments have been selected with the help of equivalent studies carried out on similar models, such as BATS, SiB, etc. Among the experiments, we have not considered the model sensitivity to bare soil albedo, because, as stated by Wilson *et al.* (1987), it has a negligible impact. Also the sensitivity to initial soil temperatures has been neglected, initial values of soil water content being far more important than initial temperatures (McCumber and Pielke, 1981; Tjernstrom, 1989). The sensitivity of LSPM to vegetation and soil characteristics has been analyzed in Carena (1998). In conclusion, the sensitivity of the LSPM model has been studied with respect to the variation of the following hydrologically related parameters (summarised in table III): initial value of soil moisture W_j^i ($j = 1, 5$) and amount of precipitation. This last simulation has been carried out by modifying only the observed precipitation rate P_0 (but not its temporal distribution) respectively in: $P_0/10$, $P_0 \cdot 10^{-0.5}$, P_0, $P_0 \cdot 10^{+0.5}$, $P_0 \cdot 10$; the exponent of the multiplying factor 10 (varying between -1 and 1) will be hereafter called precipitation code *PC*.

A peculiar methodology has been used for intial and boundary conditions. In fact, as a rule, all sensitivity studies involve fairly coarse changes in individual parameter values; often these extreme specifications are not physically realistic, but such studies serve to illustrate how land surface processes may significantly affect the atmospheric circulation (Sellers *et al.*, 1989). Then, instead of forcing the model with artificial time evolutions (such as sinusoidal functions), a set of experimental data has been used as an

---

([1]) In truth, as we have not got any direct observation of the atmosphere-ground heat flux, we evaluate it starting from the observations of soil temperature and soil heat flux (both gathered at 3 cm), by using the formula

$$G = c_p \varrho \Delta z \frac{\partial T_1}{\partial t} - \frac{\nu (T_2 - T_1)}{\Delta z} ,$$

where the term "$-\nu(T_2 - T_1)$" accounts for the measured soil heat flux at the intermediate level (in our case at 3 cm), ν is the thermal conductivity, $\Delta z = 3$ cm and $\partial T_1 / \partial t$ was obtained using the observations of the time trend of T_1 (at 3 cm as well). The numerical value used for the soil thermal capacity ϱc_p was $2.42 \cdot 10^6$ JK^{-1} m^{-3}, corresponding to a generic loam soil (see also Garratt, 1992). Even if soil moisture influences G (because ϱc_p and ν depend on soil moisture content W), as surface soil moisture values during all period of the SPCFLUX93 campaign were approximately constant, the approximation done in assuming the values of ϱc_p and ν as constant can be considered true with a good degree of accuracy. Data evaluated using the above equation were then used as "observations".

TABLE III. – *Sensitivity experiments carried out on* LSPM.

Experiment number	Parameter	Minimum value	Maximum value	Step value
1	W_j^1 ($j = 1, 5$)	0.1	0.9	0.2
2	*PC*	−1	1	0.5

input for the LSPM. In truth, we tried to use sinusoidal functions, but some difficulties occurred in the parametrization of rain and the obtained data of temperature, humidity and wind velocity were poorly correlated with solar radiation, causing unrealistic effects on the final results. Moreover, we believe that experimental data used as an input allow to determine more realistically the response of the model, and to identify its behaviour with varying input data.

Using the data-set described in the next subsection as boundary and initial conditions, in each sensitivity test we have changed only one parameter for each experiment. To analyze the results of our tests, considering that the climatic system should require a few months before forgetting the initial values of the soil moisture fields, in order to overcome these so-called "model spin-up problems" (Serafini and Sud, 1987; Milly and Dunne, 1994), we have ran the model for the entire data-set time (6 months, from January to June 1993), and considered as its output only the average values of the last month (June). A preliminar run on a longer time period (January 1993-March 1995) has been performed to demonstrate that 6 months are sufficient to overcome the " model spin-up problems". We have decided to show the results of the month of June because, in general, summer months are to be preferred in the analysis of energy fluxes and hydrological budgets for their higher variability.

5. – Boundary and initial conditions for sensitivity tests

The initial and boundary conditions used for the model in all the sensitivity experiments have been gathered at the meteorological station of San Pietro Capofiume (hereafter referred to as SPC), located about 30 km east of Bologna (Northern Italy), in the lower part of the Po Valley, at a height of 10 m above the sea level and about 100 km far from the Appennine chain. This station is located in a flat, horizontally homogeneous region, then its data could be also considered as representative of a wider region, on the mesoscale, surrounding it. A detailed description of these data follows.

5˙1. *Initial conditions.* – The soil type near the station has been assumed to belong to the class of loam, while the dominant vegetation type around the station is grass, regularly cut by the farmers. Table II reports the values of the initial conditions assumed for all the sensitivity tests.

As a result of the discussions in the appendix, in the absence of direct observations we decided to use as initial soil moisture profile the constant value $W_j^i = W_*$, $j = 1, 5$. Because the initial distribution of soil temperatures is not equally fundamental, we assigned as initial underground temperature profile the January monthly average obtained by the longer simulation (January 1993-March 1995) described in sect. **6**.

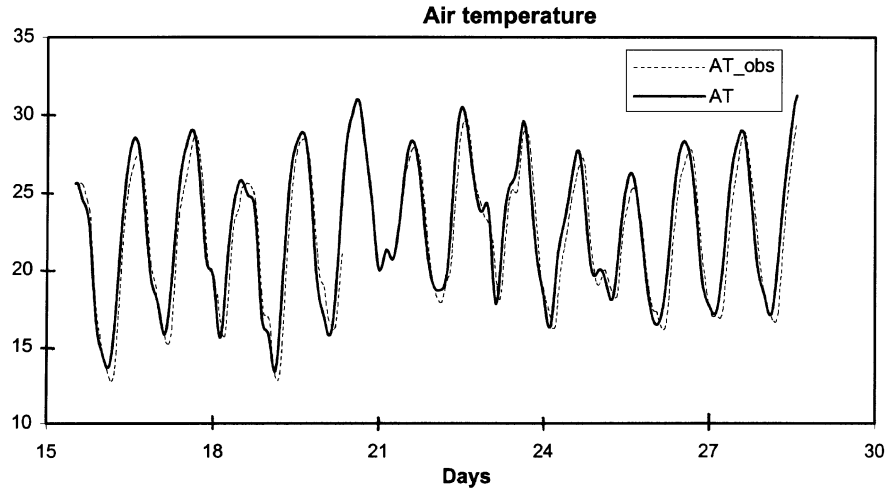

Fig. 5. – Air temperature at screen level gathered during the SPCFLUX93 experiment (dashed line) and extrapolated from synop data (solid line), in degrees.

5˙2. *Boundary conditions.* – The data used as boundary conditions come from the routine synoptic observations gathered at the WMO meteorological station of SPC. We have extracted a time period of 27 months (from January 1993 to March 1995) for each of the following data: air temperature, dew-point temperature, air pressure at the station level, precipitation, total and low-level cloudiness, wind velocity. Original data were available every 3 hours (from 00 UTC) with the exception of precipitation data, that has been treated separately, as discussed later on in this section.

All synop data (but precipitation) were interpolated with cubic spline functions (from "Numerical Recipes", Press *et al.*, 1988), in such a way to get input data every 30 minutes.

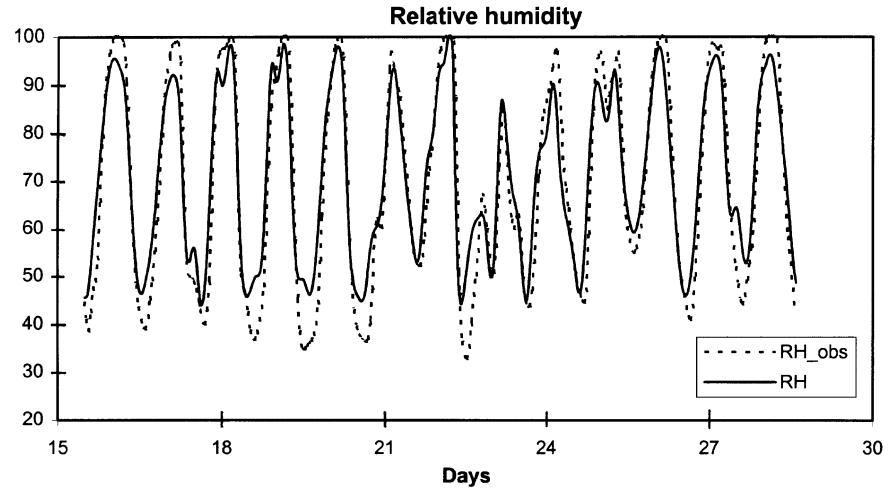

Fig. 6. – Same as fig. 1 but for relative humidity, in percent.

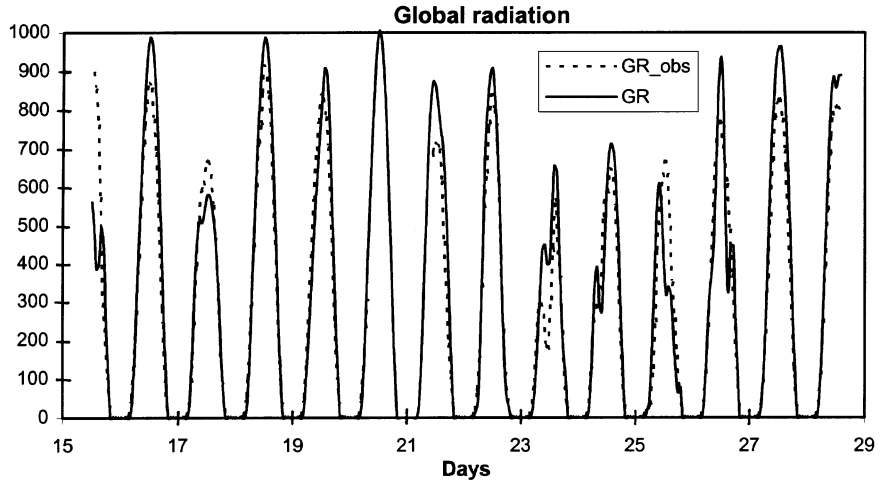

Fig. 7. – Same as fig. 1 but for the global solar radiation, in Wm^{-2}. The solid line refers to the LSPM output data.

Since synoptic observations of the wind refer to an anemometer installed at 10 m above the soil surface, while LSPM needs a wind at the reference height (z_a), the synop wind data has been devided by a factor of $\sqrt{2}$ to reduce them at z_a height. This factor has been determined experimentally by the comparison of the synop data with the observations relative to the experimental campaign SPCFLUX93 (Cassardo *et al.*, 1998), performed in a grass field near the synoptic station of SPC from 15th to 28th June 1993. This assumption is also compatible with the hypothesis of a neutral logarithmic wind profile with a roughness length $z_0 \simeq 0.01$ m (realistic value for short grass).

Regarding precipitation, a rearrangement of synop messages referring to the hours

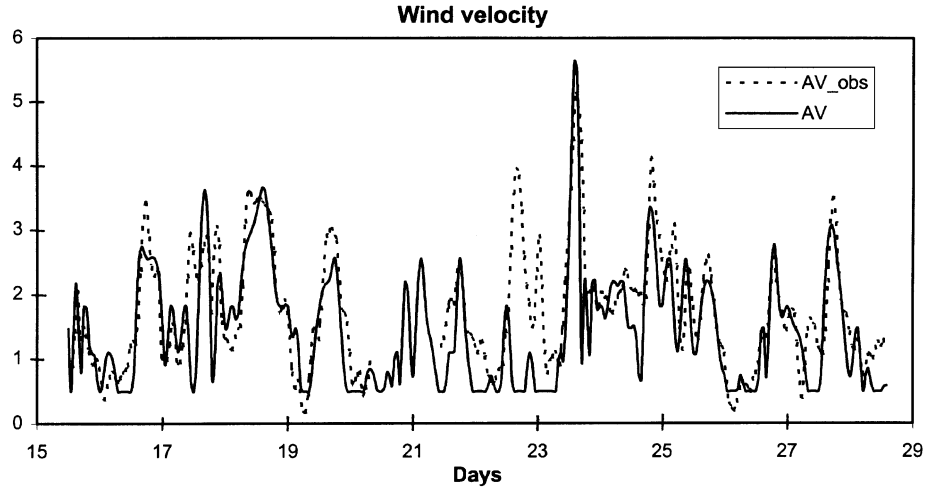

Fig. 8. – Same as fig. 1 but for horizontal wind velocity, in ms^{-1}.

00, 06, 12 and 18 UTC gives us the precipitation relative to the six hours preceding the observation; to obtain data every 30 minutes, we have equally distributed the six-hourly amount of precipitation in sub-intervals of 30 minutes.

As to the boundary condition for the bottom soil layer, for the thermal component the condition of null bottom flux has been used: for long-time simulations, it is to be preferred to the condition of fixed temperature (Warrilow *et al.*, 1986). For the soil moisture, the capillarity rise has been neglected (as we consider locations far from coastal regions), while the gravitational drainage has been parametrized, as explained in subsect. **2**·3.

5·3. *Verification of the boundary conditions parametrizations.* – As the original input data have been "worked in", some errors could have been included due to rearrangement of the data themselves; therefore, we checked the quality of our data by comparing them with those obtained during the experimental campaign SPCFLUX93 ([2]).

We decided to compare also the solar global radiation, since this last quantity is calculated by LSPM by using the observed total and low-level cloudiness with a rearrangement of the algorithm described in Page (1986).

In figs. 5 to 9 we have reported the trends of temperature, relative humidity, wind velocity, precipitation and global radiation, respectively, for the whole period of the SPCFLUX93 campaign; rearranged synop data are shown by solid lines and SPCFLUX93 data by dashed lines. As can be seen, there is a good agreement between the input data after our "treatment" and the direct observations for temperature (fig. 5), relative humidity (fig. 6, with some imprecisions in daytime minima) and global radiation (fig. 7); there is a satisfactory agreement for wind velocity (fig. 8, except day 22nd), while the precipitation distribution (fig. 9) is smoothed (the total

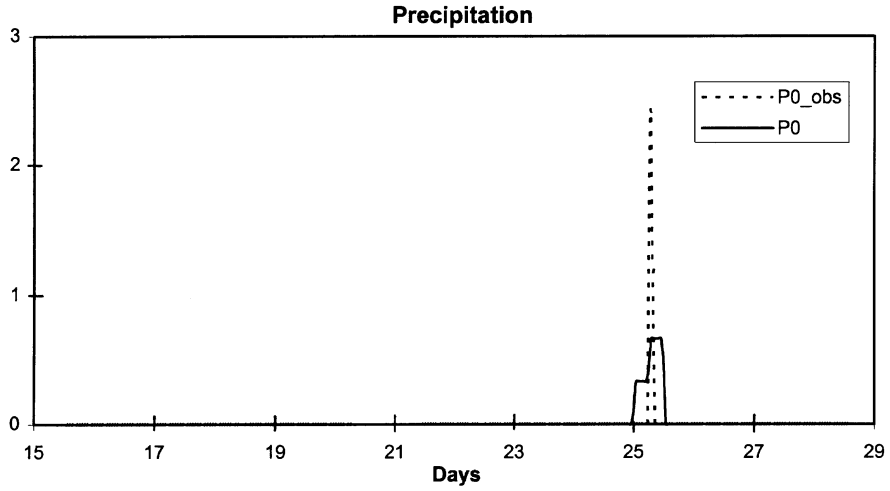

Fig. 9. – Same as fig. 1 but for cumulated half-hour precipitation, in mm.

([2]) For a more complete review of the instruments installed during this experiment we are preparing a report (Cassardo *et al.*, 1998); a description of the campaign is already available in Italian (Manzi *et al.*, 1994) and is briefly reviewed in Cassardo *et al.* (1995b).

amount being correct): we shall reserve to a future work the use of some distribution functions for the precipitation.

We can conclude this section by pointing out that our interpolation method on synop data has allowed us to derive good quality data to be used as an input for LSPM.

6. – Results and discussion on the sensitivity experiments

A preliminary simulation run was performed to check whether during the first five months of simulation the model had reached the equilibrium regime (in other words, if the so-called "spin-up problems" had been overcome). This preliminary run started at the same time of the sensitivity experiments (*i.e.* 1st January 1993) but it lasted 2 years and 3 months (up to March 1995). LSPM initial and boundary conditions were the same for all the sensitivity experiments (table III).

6˙1. *Experiment 1: Preliminary simulation and results of long-term run.* – In fig. 10 we present the monthly cumulated values (in mm) of evapotranspiration (LE), precipitation (P_0), runoff (r_s) and drainage (r_u), and the monthly averaged total soil water content (*water*, in cm): we can deduce that in 1993 the precipitation was lower than in 1994, and that the total soil water content in the winters 1993-94 and 1994-95 was of the same order of magnitude as the initial value. This fact is confirmed by observing the distribution of soil moisture (monthly averaged values, in fig. 11); we can observe that in January (1993, 1994 and 1995) the mean values of the soil moistures are similar at all levels, and close to the "deep soil moisture threshold" W_* (appendix).

We can then infer that the yearly hydrologic cycle is realistic, and then it is reasonable to use the June 1993 mean values in the sensitivity experiments. Then, for both experiments we shall analyze the monthly averages relative to the June month only. The model's results are reported in tables IV-V, while only the more representative graphs are shown and commented.

6˙2. *Experiment 2: Model sensitivity to initial soil moisture.* – As commonly known, initial soil moisture is perhaps the most important parameter in the short-term forecast. The degree of soil saturation influences the partitioning of the outgoing

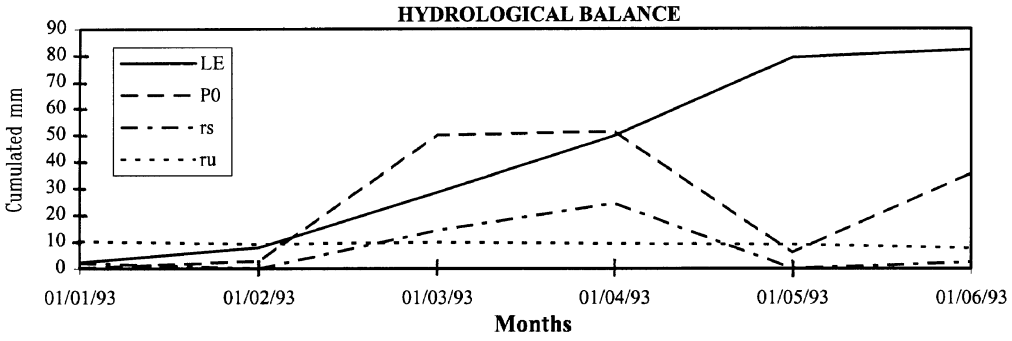

Fig. 10. – Monthly cumulated values (in mm) of evapotranspiration (LE), precipitation (P_0), runoff (r_s) and drainage (r_u), and monthly average (in cm) total soil water content (water) during long-time simulation.

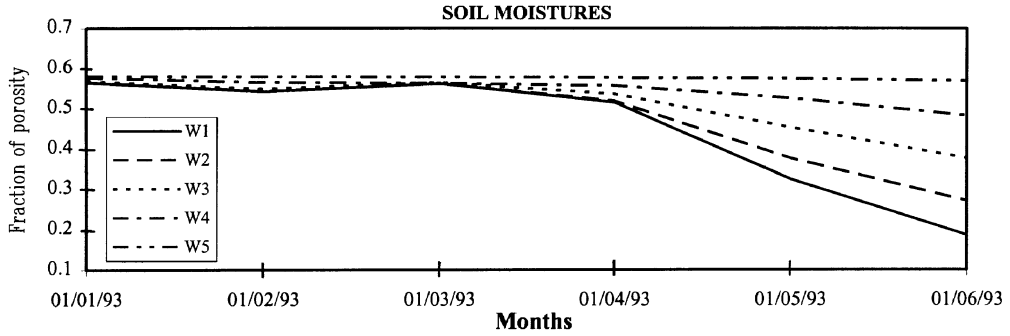

Fig. 11. – Monthly average values of relative soil moisture (W_1–W_5) during long-time simulation, in percent.

energy between the latent and sensible heat fluxes. Interactive soil moisture allows larger variations of these fluxes, thereby increasing the variance of the surface air temperature. Because latent heat flux (under conditions of sufficiently high soil

TABLE IV. – *Summary of monthly averaged values for June* 1993 *relative to the sensitivity experiment on initial soil moisture.*

W_j^i, $j = 1, 5$	0.1	0.3	0.5	0.7	0.9
RN (Wm^{-2})	141	142	149	157	158
H (Wm^{-2})	116	112	89	66	62
LE (Wm^{-2})	39	43	70	93	96
QG (Wm^{-2})	3	3	5	6	7
TR (Wm^{-2})	34	39	64	79	82
EFW (Wm^{-2})	12	12	11	11	11
EG (Wm^{-2})	−6	−7	−6	3	3
LE (mm)	39	44	70	94	97
P_0 (mm)	36	36	36	36	36
r_s (mm)	1	1	1	1	1
r_u (mm)	0	0	1	26	46
T_1 (°C)	30.5	30.3	29.0	26.8	26.7
T_2 (°C)	29.4	28.9	26.8	25.5	25.6
T_3 (°C)	25.6	24.0	23.2	23.0	23.2
T_4 (°C)	13.1	14.2	16.9	17.5	17.6
T_5 (°C)	10.0	11.4	10.3	9.8	9.7
T_c (°C)	27.6	27.4	26.4	25.5	25.4
W_1	0.14	0.12	0.17	0.29	0.34
W_2	0.11	0.15	0.25	0.35	0.38
W_3	0.18	0.24	0.35	0.43	0.46
W_4	0.10	0.30	0.46	0.52	0.54
W_5	0.10	0.30	0.50	0.62	0.65
r_a (sm^{-1})	83	86	97	102	96
r_b (sm^{-1})	19	19	19	19	19
r_c (sm^{-1})	3 500	3 120	2 220	1 990	1 960
r_d (sm^{-1})	51 800	54 500	64 900	69 400	63 600
r_{soil} (sm^{-1})	12 300	19 000	10 500	5 920	5 100

TABLE V. – *Summary of monthly averaged values for June* 1993 *relative to the sensitivity experiment on amount of precipitation* (*PC varying from* −1 *to* 1).

PC	−1	−0.5	0	0.5	1
RN (Wm^{-2})	144	146	154	161	162
H (Wm^{-2})	104	96	73	56	53
LE (Wm^{-2})	51	60	85	105	107
QG (Wm^{-2})	6	6	6	8	9
TR (Wm^{-2})	58	62	73	88	89
EFW (Wm^{-2})	3	7	11	13	14
EG (Wm^{-2})	−10	−8	1	4	4
LE (mm)	52	61	86	106	108
P_0 (mm)	4	11	36	113	356
r_s (mm)	0	0	1	18	178
r_u (mm)	7	7	8	18	50
T_1 (°C)	30.1	29.5	27.4	26.5	26.3
T_2 (°C)	27.4	26.9	25.6	25.9	25.9
T_3 (°C)	23.1	22.9	22.9	24.2	24.4
T_4 (°C)	16.3	16.5	17.3	19.0	19.4
T_5 (°C)	9.7	9.9	10.1	9.9	10.1
T_c (°C)	27.1	26.8	25.8	25.2	25.1
W_1	0.10	0.13	0.23	0.51	0.61
W_2	0.22	0.23	0.31	0.52	0.61
W_3	0.35	0.36	0.40	0.55	0.62
W_4	0.47	0.47	0.50	0.57	0.62
W_5	0.56	0.56	0.57	0.61	0.65
r_a (sm^{-1})	93	96	108	85	84
r_b (sm^{-1})	19	19	19	19	19
r_c (sm^{-1})	2 360	2 280	2 060	1 900	1 890
r_d (sm^{-1})	61 600	63 800	75 000	52 800	52 100
r_{soil} (sm^{-1})	13 900	11 900	7 450	3 760	3 340

moisture) is proportional to potential evaporation, the greatest influence of soil moisture on the atmosphere is when potential evaporation values are larger, *i.e.* in the tropics and summer hemisphere extra tropics (Delworth and Manabe, 1988).

There are many reasons for which it is important to test the model ability to predict correctly the hydrological budget. From a physical point of view, the vertical profiles of surface latent and sensible heat fluxes influence convection, cloudiness, radiation and precipitation processes. On the other hand, the knowledge of the amount of soil water content permits to assess when the plant reaches its physiological limits (due to drought conditions), or if irrigation is necessary, or even the compatibility of a particular kind of canopy with the soil water regime of a determined region. Finally, the knowledge of the soil water content is necessary to predict the retention capacity of the soil and then the amount of water released in strong precipitation events.

Figure 12 shows the energy balance. Net radiation (*RN*) increases by 17 Wm^{-2} with the growth of initial soil moisture W_j^i, $j = 1, 5$ (hereafter referred to simply as W_j^i) from 0.1 to 0.9. As expected, the turbulent heat fluxes are the physical quantities mainly affected by this variation of W_j^i: for low W_j^i, sensible heat flux (*H*) is about 3 times

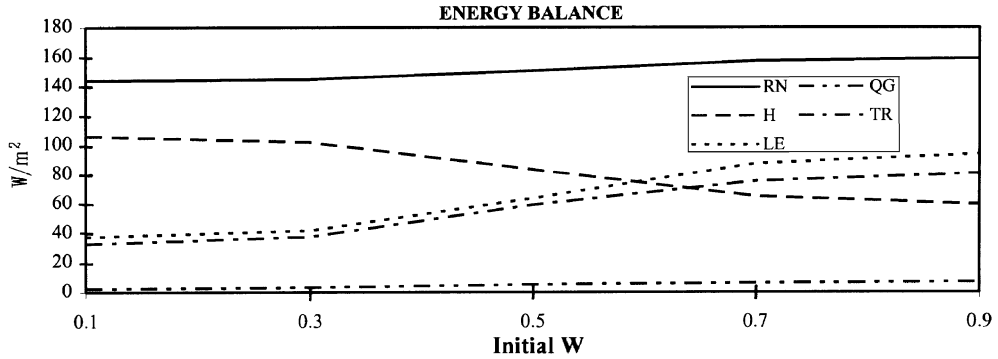

Fig. 12. – Sensitivity experiment on initial soil moisture content. June monthly values of: net radiation (RN), sensible (H), latent (LE) and conductive (QG) heat fluxes, and transpiration (TR), all quantities in Wm^{-2}.

greater than the latent one (LE), while at higher values of W_j^i, LE is greater than H, due to the high values of canopy and soil resistances (table IV), being around $W_j^i \cong 0.6$ the value of W_j^i at which $H \cong LE$. QG slowly grows with increasing W_j^i (because the soil thermal conductivity increases by about one order of magnitude as W_j^i increases from 0.1 to 0.9), but its monthly average is always a negligible part of the total energy budget; for the same reason, in the simulations with higher W_j^i the soil temperature is more influenced by the yearly surface thermal wave. The soil surface temperature T_1 tends to decrease (table IV) when the moisture content is higher, as also observed by Wilson *et al.* (1987).

Figure 13 reports the soil moisture trends in the five soil layers. It is interesting to note the different degree of soil wetness depending on the initial values W_j^i: for $W_j^i = 0.1$ only the upper three layers are wet by precipitation; as the "effective" precipitation cumulated over all the integration period January-June (*i.e.* the precipitation reaching the soil, given by $P_0 - r_s$: about 140 mm) is larger than the cumulated evaporation (about 130 mm), the first layer is wetter than the second. The wettest layer is the third

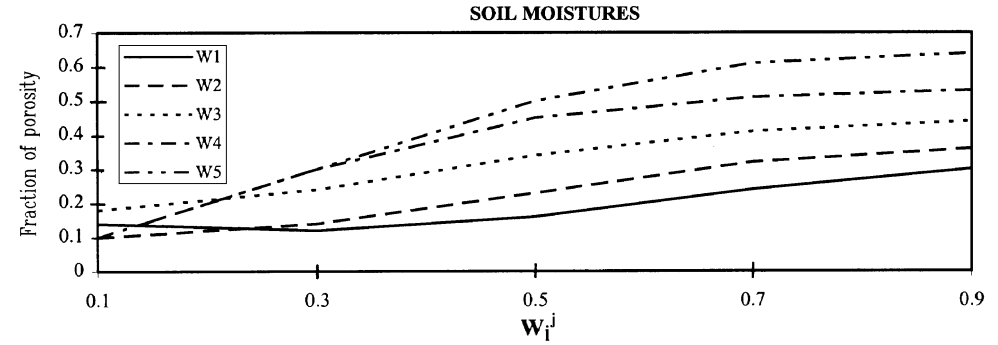

Fig. 13. – Same as fig. 12 but for soil moistures (W_1–W_5), expressed in percent.

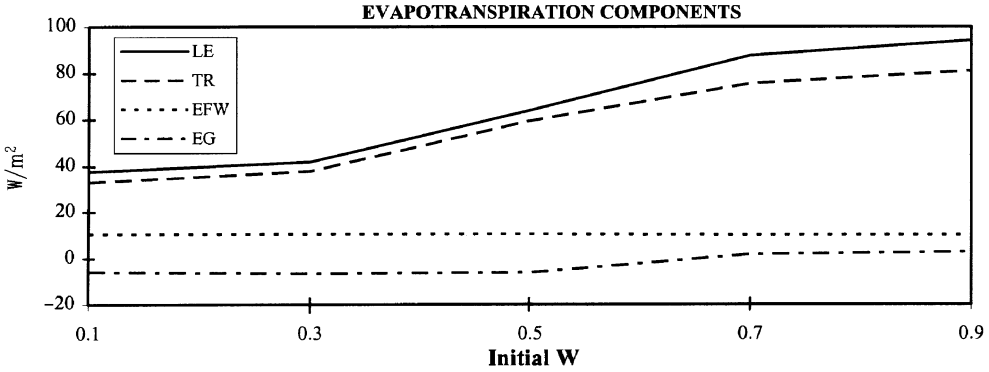

Fig. 14. – Same as fig. 12 but for evapotranspiration (*LE*), transpiration (*TR*), evaporation from wet fraction of canopy (*EFW*) and from bare soil (*EG*), all in Wm^{-2}.

one: this peculiar moisture distribution into the soil is due to three factors: the transfer velocity of water into soil is low for dry soils, so the water moves slowly into the terrain; the evapotranspiration acts only on the first two layers of soil for the canopy type (short grass) used in these simulations; and the actual temporal distribution of the observed precipitation in the six months of simulation (fig. 10) was irregular, with the maxima in early spring (March and April) and some peaks in June, due to thunderstorms or showers, alternating with long sunny dry periods. For $W_j^i = 0.3$ the distribution of soil moisture is monotone and the first soil layers is drier than the second one, because in this case the six month cumulated evaporation (about 170 mm) is higher than the "effective" precipitation (about 140 mm). For W_j^i 0.5 too, the evaporation is much larger than the effective precipitation and the first layer is the driest; furthermore, as the bottom drainage r_u (table IV) reaches high values (46 mm for $W_j^i = 0.9$), the hydrological balance is therefore negative and this fact explains the significant difference of soil moisture from the initial value.

Regarding the evapotranspiration, the relative importance of all its terms can be inferred by examining fig. 14. The evaporation from the wet canopy fraction *EFW* (mainly depending on vegetation cover and amount of precipitation) is practically constant. The transpiration *TR* is the dominant term and represents about 80% of the total *LE*; the bare soil evaporation *EG* is positive for $W_j^i \geqslant 0.7$, while for lower W_j^i it is negative, meaning that the soil is wetter than the atmosphere (and the canopy), according to the considerations of subsect. **5**˙2.

6˙3. *Experiment 3: Model sensitivity to amount of precipitation.* – This experiment has been carried out in order to verify the model response to changes in one of the fundamental input quantities, *i.e.* the amount of precipitation. We will again point out that, in this experiment, we have only stretched or shrinked the observed precipitation P_0 by using factors of $10^{0.5}$ (*i.e.* about 3.2) and 10, without changing its temporal distribution, so this can be considered a sensitivity experiment on rainfall intensity. The value $10\,P_0$ (corresponding to an average precipitation of 10 000 mm y^{-1}) can be considered as representative of extreme rainfall conditions, while $10^{-1}P_0$ (corresponding to 100 mm y^{-1}) can be considered as a typical value for arid conditions.

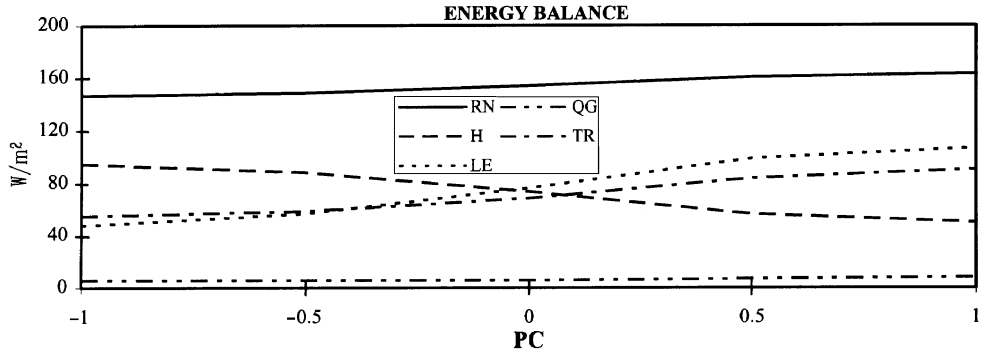

Fig. 15. – Same as fig. 12 but for the sensitivity experiment on the amount of precipitation. *PC* is defined as the exponent of the multiplying factor 10 applied at the observed data.

We wish to remark here that the above modifications in the precipitation regime can even produce strong changes into the climatic system and that conclusions resulting from the output must be regarded cautiously. In any case, however, as we want to analyze the effects of the different amount of precipitation on the global hydrologic cycle, we found that in this case our method gives more realistic results with respect to the use of prescribed atmospheric forcings. All the results of these tests are listed in table V.

In fig. 15 we report the energy balance: *RN* increases by about 20 Wm^{-2} when the precipitation code *PC* grows from -1 to 1; *QG* is approximately constant, while turbulent heat fluxes have opposite trends, *LE* being larger with high PC. *TR* is a large fraction of *LE* and, for low *PC*, tends to be larger than *LE*, indicating that, in this extreme case, the plants tend to absorb the water vapour directly and more easily from the atmosphere rather than from the dry soil. As a consequence, for $PC = -1$, EG is about -10 Wm^{-2} (table V).

Figure 16 shows the trend of soil moistures: the main variations affect mainly the upper three layers, W_5 remaining practically constant. For $PC > 0$ all soil layers are above the wilting point even in summer, while for $PC < 0$ the moisture in the root zone

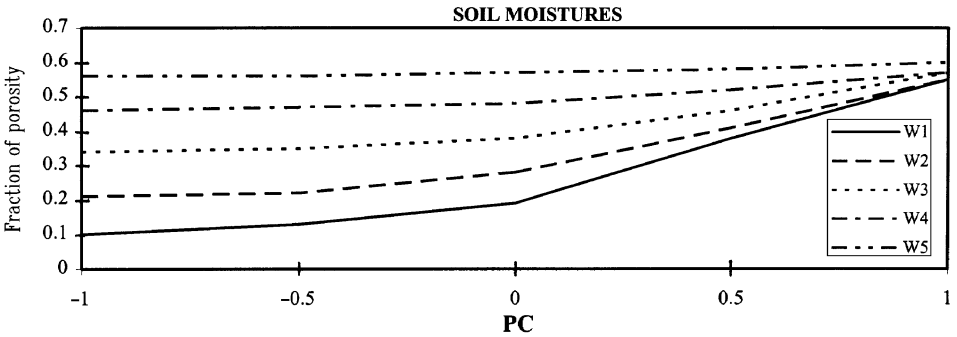

Fig. 16. – Same as fig. 13 but for the sensitivity experiment on the amount of precipitation. *PC* is defined as in fig. 15.

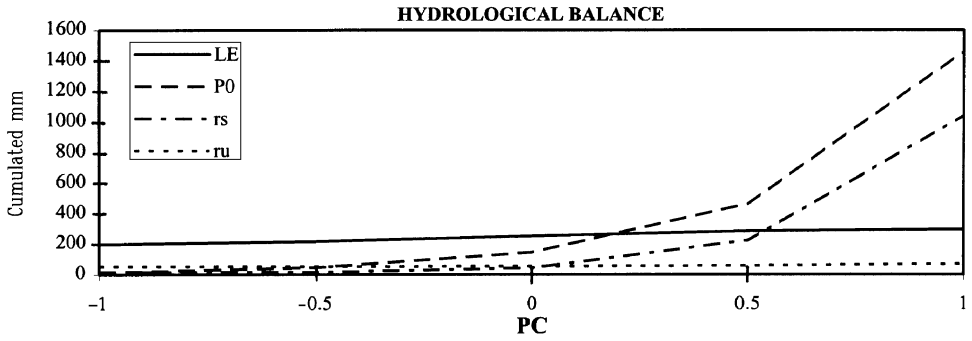

Fig. 17. – Sensitivity experiment on the amount of precipitation. June monthly cumulated values of: evapotranspiration (LE), precipitation (P_0), runoff (r_s) and drainage (r_u), expressed in monthly cumulated mm. PC is defined as in fig. 15.

(first two layers) could cause the death of this canopy type. Correspondingly, canopy and soil surface temperatures are higher for $PC = -1$.

Finally, fig. 17 reports the hydrological budget: as expected, the largest variations due to changes in the amount of precipitation mainly affect the surface runoff; when the precipitation varies between 4 and 356 mm, r_s grows from 0 (for $PC = -1$) to 178 mm (for $PC = 1$).

For all quantities, the largest variations happen between $PC = -0.5$ to $PC = 0.5$, indicating that below or above this threshold level, the amount of rainfall does not influence further the balances.

7. – Conclusions

In the present work, some validation and sensitivity tests performed on LSPM (Land Surface Process Model of Cassardo *et al.*, 1995a) have been presented and discussed. The validation has been applied to the observations gathered during a field experiment carried out at Mottarone (Verbania, Northern Italy). The selected parameters for our sensitivity tests have been two hydrologically related important parameters: initial soil moisture in all soil layers of the model and amount of precipitation.

The response of the LSPM to all these simulations appeared to be satisfactory: the model seemed to reproduce the trends of energy, thermal and hydrologic budgets with an accuracy comparable with the one inferred by the examination of climatological considerations or found in similar tests performed by other researchers on other models. In particular, some interesting results can be mentioned:

a) the apportionment between sensible and latent heat fluxes is close to the observations, even if the evapotranspiration is a little underestimated; the net radiation is well represented, suggesting that the radiative part of LSPM, in spite of its simplicity, gives results of excellent quality;

b) the simple method used for the interpolation of synop data as boundary conditions has been succesfully tested by comparing its predictions with independent experimental observations;

c) the method of initializing the "deep soil moisture" proposed in the appendix seems to produce reasonable results if the run starts in winter conditions and can be applied in all cases in which the precipitation regime is normal;

d) the LSPM output does not show any substantial changes when the precipitation is 3 times larger than the standard precipitation or is lower than one-third of it.

* * *

The authors wish to thank C. CACCIAMANI of SMR-ER (Regional Meteorological Service of Emilia Romagna, Bologna, Italy) for helping in the development of the software for the treatment of synop data, the SMR-ER for allowing the use of synop data, G. MANZI of ENEL-CRAM (Milan, Italy) for the help in the extraction of data from the SPCFLUX93 campaign database and P. M. RUTI of ENEA (Rome, Italy) for the useful discussions on the subject of the present work. This work has been partially supported by CNR-ENEL Research Contract "Interazione dei sistemi energetici con la salute dell'uomo e dell'ambiente", Sub-Project 3, Line 2.4 and by the World Laboratory, Land Project 2 no. 305, Lausanne.

APPENDIX

Determination of initial deep soil moisture in winter

As summarised in subsects. **6**·2 and **6**·3, there is an evident correlation between soil moisture in the lowest model layer W_5 and underground drainage r_u: if the cumulated monthly value of r_u is $\leqslant 10$ mm, W_5 monthly variation is less than 1%. If we impose a fixed monthly value of drainage $r_u^* = 10$ mm as a "threshold" value, if $r_u < r_u^*$ the drainage is too low to produce a noticeable change in the soil water content (in the absence of input from upper levels), while if $r_u > r_u^*$ the drainage increases and correspondingly the soil water content decreases. It is then possible to determine

TABLE VI. – *List of "thresold" values for deep soil moisture.*

ST	*W**
1	0.38
2	0.41
3	0.49
4	0.57
5	0.58
6	0.65
7	0.72
8	0.72
9	0.77
10	0.79
11	0.80
12	0.66

the soil moisture value W_* corresponding to r_u^*, (by using a time interval $\Delta t = 2.592 \cdot 10^6$ s, corresponding to one month); such values are reported in table VI.

As shown in subsect. **6**·5, the monthly average of the deep soil moisture W_5 diverges from W_* by only a few percent in the normal precipitation range (*i.e.* for $-0.5 \leqslant PC \leqslant 0.5$ in table V) and for each soil type (Carena *et al.*, 1998); for soils 6–12 the initial values of soil moisture were too low with respect to W_*.

The value of W_* can then provide an estimate of the soil moisture in the deepest layers under standard precipitation conditions. Regarding the distribution of soil moisture in the highest layers, it is necessary to take into account many factors, *i.e.* vegetation, precipitation history, season, latitude, wind regime, soil type, etc. For climatological purposes, nevertheless, it is convenient to start the simulations in winter conditions: in fact, the evapotranspiration is lower in winter than in summer (then, also the soil moisture gradient is lower than in summer), and the surface soil moisture depends mainly on precipitation regime and on soil type. In middle latitude regions (where the canopy is subject to the yearly cycle or where the forests are broadleaf) and under normal conditions of precipitation, we can suppose that we do not make a significative error if we consider the initial soil moisture as a constant (equal to W_*) in all soil layers, as can also be inferred by examining fig. 11, in which the monthly averaged values of January soil moistures did not substantially depart, in all layers, from the constant vertical distribution $W = W_*$.

REFERENCES

ABRAMOPULOS F., ROSENZWEIG C. and CHOUDHURY B., *J. Climate*, **1** (1988) 921-941.

BELJAARS A. C. M. and VITERBO P., *Boundary-Layer Meteorol.*, **71** (1994) 135-149.

BOSILOVICH M. G. and SUN W. Y., *Boundary-Layer Meteorol.*, **73** (1995) 321-341.

CARENA E., CASSARDO C. and LONGHETTO A., submitted to *Boundary-Layer Meteorol.*, (1998).

CASSARDO C., JI J. J. and LONGHETTO A., *Boundary-Layer Meteorol.*, **72** (1995a) 87-121.

CASSARDO C., SACCHETTI D., MORSELLI M. G., ANFOSSI D., BRUSASCA G. and LONGHETTO A., *Nuovo Cimento C*, **18** (1995b) 419-440.

CASSARDO C., BRUSASCA G., FERRARESE S., FERRERO E., GIRAUD C., LONGHETTO A., MANZI G., and MORSELLI M. G., *San Pietro Capofiume 1993 (SPCFLUX93) experimental campaign in Atmospheric Boundary Layer. Preliminary Results*, in preparation (available from authors as internal report of MANZI *et al.*, 1994, in these references, in Italian) (1998).

CLAPP R. B. and HORNBERGER G. M., *Water Resour. Res.*, **14** (1978) 601-604.

DEARDOFF J. W., *J. Geophys. Res. C*, **83** (1978) 1889-1903.

DELWORTH T. L. and MANABE S., *J. Climate*, **1** (1988) 523-547.

DICKINSON R. E., HENDERSON-SELLERS A., KENNEDY P. J., and WILSON M. F., *Biosphere-Atmosphere Transfer Scheme (BATS) for the NCAR Community Climate Model*, *NCAR Tech. Note*, NCAR/TN-Z75 str. Boulder, Colorado (1986).

DINGMAN S. L., in *Physical Hydrology* (Macmillan College Publishing Company, New York) 1994.

EK M. and CUENCA R. H., *Boundary-Layer Meteorol.*, **70** (1994) 369-383.

GARRATT J., in *The Atmospheric Boundary Layer* (Cambridge University Press) 1992.

HENDERSON-SELLERS A. and PITMAN A. J., *J. Geophys. Res. D*, **97** (1992) 2687-2696.

HENDERSON-SELLERS A., YANG Z. L. and DICKINSON R. E., *Bull. Am. Meteorol. Soc.*, **74** (1993) 1335-1349.

JACQUEMIN B. and NOILHAN J., *Boundary-Layer Meteorol.*, **52** (1990) 93-134.

MANLEY R. E., *J. Hydrol.*, **35** (1977) 341-356.

MANZI G., GALOFARO D., MORSELLI M. G. and BRUSASCA G., *S. Pietro Capofiume campaign, June 1993*, ENEL CRAM Internal Report (in Italian), E1/94/04, Milano, Italy (1994).

MCCUMBER M. and PIELKE R. A., *J. Geophys. Res. C*, **86** (1981) 9929-9938.

MILLY P. C. D. and DUNNE K. A., *J. Climate*, **7** (1994) 506-514.
PAGE J. K., in *Prediction of Solar Radiation on Inclined Surfaces*, edited by J. K. PAGE (D. Reidel Publishing Company) 1986.
PRESS W. H., TEUCOLSKY S. A., VETTERLING W. T. and FLANNERY P. P., in *Numerical Recipes* (Cambridge University Press, Cambridge, UK) 1988.
RUTI P. M., CASSARDO C., CACCIAMANI C., PACCAGNELLA T., LONGHETTO A. and BARGAGLI A., *Intercomparison between BATS and LSPM surface schemes, using point micrometeorological data set*, *Beitr. Phys. Atm.*, **70** (1997) 201-220.
SELLERS P. J., MINTZ Y., SUD Y. C., and DALCHER A., *J. Atmos. Sci*., **43** (1986) 505-531.
SELLERS P. J., SHUTTLEWORTH J., DORMAN J. L., DALCHER A., and ROBERTS J. M., *J. Appl. Meteorol.*, **28** (1989) 727-759.
SERAFINI Y. V. and SUD Y. C., *J. Climatol.*, **7** (1987) 585-591.
TJERNSTROM M., *Boundary-Layer Meteorol.*, **48** (1989) 33-68.
VERSTRAETE M. M. and DICKINSON R. E., *Ann. Geophys. B*, **4** (1986) 357-364.
VITERBO P. and BELJAARS A. C. M., *J. Climate*, **8** (1995) 2716-2738.
WARRILOW D. A., SANGSTER A. B. and SLINGO A., *Modelling of land surface processes and their influence on European climate*, *Tech. note no. 38* (UK Meteorol. Office) 1986.
WILSON M. F., HENDERSON-SELLERS A., DICKINSON R. E., and KENNEDY P. J., *J. Clim. Appl. Meteorol*., **26** (1987) 341-362.
ZHANG T. P., *J. Climate.*, **7** (1994) 890-913.